

## **Corrosion Behavior of Electroless Nickel Coatings in Concentrated Salt Solutions**

Sudarshan Lal  
FCI Electronics (USA), Inc.

### **Abstract**

Electrical connectors require durable housings made of economically feasible materials. Often, appropriate surface finishes are required for increased durability in service environments. The present study was initiated to select a suitable surface finish that would withstand high salt and humidity-laden environments for extended periods of time. This paper summarizes corrosion results on different finishes in the presence of selected electrolytes. Electroless nickel coatings of varying phosphorous content are compared with electroplated nickel on 301 stainless steel substrate. The role of electrochemical and galvanic behavior on select coatings was also considered.

For more information, contact:

S. Lal  
FCI Electronics (USA), Inc.  
320 Busser Road  
Emigsville, PA 17318-0248  
Phone: 717-764-7328; Fax: 717-764-7103  
E-mail: [slal@fciconnect.com](mailto:slal@fciconnect.com)

## **Introduction**

Metallic raw materials such as copper alloys, aluminum, and steels are often specified in designing connector terminals and their housings. Some applications are stamp and ship and some applications are comprised of stamping, plating and shipping. The latter class of products require acceptable metallic coatings in order to combat the wrath of corrosion which is a warranted evil. However, with judicious care and selection of the right coatings, the corrosion process can be minimized to obtain a useful service life. Thus, the bare substrates are coated with metallic finishes to preserve the integrity and functionality of the base materials. In this work, we describe the case history of developing a housing for a connector that was susceptible to a salt laden and humid environment and the specification called for base material of stainless steel 301 or SS 303. The qualification requirement was that the coating should withstand 500 hours of neutral salt spray. This paper presents the corrosion behavior of electroless nickel (varying P content) and electroplated nickel coatings in 5 % neutral sodium chloride and some other selected electrolytes. Electrochemical polarization studies for these deposits in concentrated electrolytes has been examined in detail. The present data was helpful to the product engineer for

recommending a given coating for the desired function qualification.

## **Experimental**

Copper alloy, phosphor bronze 510 (1"x1" inch, 0.012" thick) with total area 0.014 sq. ft. were degreased with acetone, methanol and were cathodically cleaned in a proprietary alkaline cleaner. These samples were activated in 10% H<sub>2</sub>SO<sub>4</sub> and electroplated in a sulfamate nickel bath for varying nickel thicknesses. Nickel coatings of varying thicknesses and varying phosphorous contents were also prepared from commercially available chemistries. For processing phosphor bronze 510, the coupons were soak- cleaned, electrocleaned, and activated in 30% HCl.

Stainless steel 301 coupons 1" x 1" dimension were degreased in acetone and methanol, and were cathodically and anodically electrocleaned in an alkaline cleaner activated in 30% HCl cathodically and electroless nickel (EN) plated with cathodic initiation with low, medium, and high phosphorous electroless nickel. The EN process was especially suitable for parts with any recessed surfaces that were difficult to electroplate uniformly. For parts with complex geometry, after following the specified process sequence, the parts were subjected to Wood's Nickel strike (to ensure adhesion) prior to immersion in

electroless nickel bath. Three proprietary EN baths were employed for obtaining deposits with low, medium, and high phosphorous levels.

Corrosion potentials and electrochemical polarization curves were obtained using a microprocessor controlled, Potentiostat/Galvanostat apparatus in conjunction with a flat cell equipped with a three-electrode system. All applied potentials were recorded vs. Ag/AgCl reference electrode. The test solutions were prepared from analytical grade reagents. The electrolytes tested were not de-aerated and all electrochemical tests were carried out in a glass cell at 25°C as per ASTM methods<sup>1-4</sup>. Cleaned test coupons were mounted in the flat cell (effective exposed area = 1 cm<sup>2</sup>) and immersed in the solution for 15-20 minutes until a steady state corrosion potential ( $E_{corr}$ ) was obtained. The electrochemical potentials were measured with a high impedance electronic voltmeter and a capillary probe placed between reference electrode and the metal surface for least iR drop. A Potentiostat was used to impose a constant potential difference between the specimen and the reference electrode. On obtaining the steady state condition, polarization was initiated at -250 mV relative to  $E_{corr}$ , followed by a forward scan towards the noble direction at a rate of 1 mV/sec. From the knowledge of corrosion currents, and Tafel slopes<sup>5</sup>, the corrosion rates<sup>6-8</sup> were calculated from equations (a) and (b).

$$I_{CORR} = \frac{\beta_a \beta_c}{2.3(\beta_a + \beta_c)} x \frac{\Delta I}{\Delta E}$$

(a)

$$Corr. Rate(mpy) = 0.13 x I_{CORR} x \frac{Eq. Wt.}{\rho}$$

(b)

In these equation (a) and (b),  $\beta_a$  and  $\beta_c$  are Tafel slopes of anodic and cathodic polarization curves and  $\rho$  is the alloy density (g/cc).

The electrochemical techniques comprised of recording corrosion potentials  $E_{corr}$ , Tafel plots, Potentiodynamic polarization curves and Cyclic polarization plots. For galvanic corrosion<sup>9</sup> experiments, the flat cell was modified by replacing the auxiliary electrode with another coupon with a dissimilar coating and corrosion current was monitored for a given metal couple in a selected electrolyte.

Salt spray testing<sup>3</sup> in neutral 5 % sodium chloride was also performed on these coatings for extended periods of exposure time ranging from 24 hours to 500 hours in order to acquire long term corrosion data. All solutions were prepared in de-ionized water. ACS analytical reagent grade chemicals were employed in this study and pH adjustments were made by addition of 1N HCl or 1N NaOH solutions.

SEM examinations and photomicrographs of the specimens were obtained to reveal the corrosion characteristics. Analysis of solutions for metals was done by atomic absorption spectroscopy (AAS) in order to understand the corrosion mechanisms. Coating thicknesses were monitored by X-ray Fluorescence Spectroscopy.

## **Results and Discussion**

### **A) Electrochemical Tests**

The electrochemical corrosion results of electroless and electroplated nickel coatings and base materials in 5% neutral NaCl ( pH = 6.8 ) are summarized in Table I.

**Table I**  
Nickel Coatings in 5% NaCl

Coating Type*	$E_{\text{corr}}$ vs. Ag/AgCl, V	$I_{\text{corr}}$ , $\mu\text{a}/\text{cm}^2$	C. R., mpy
EN-A1	-0.250	12.4	5.43
EN-A2	-0.253	6.1	2.67
EN-B1	-0.274	5.4	2.30
EN-B2	-0.278	1.3	0.55
EN-C1	-0.284	2.9	1.33
EN-C2	-0.295	1.2	0.55
EL-Ni	-0.165	0.8	0.35
EL-Ni	-0.105	0.5	0.28
SS 301	-0.248	1.1	0.50
Ph.Br 510	-0.174	1.8	0.85

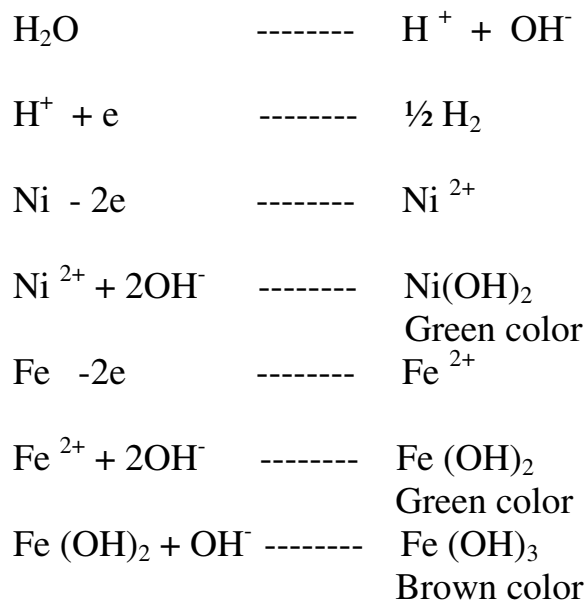
\* EN-A contains 2-4% P, 0.5 and 1.0 mil thick  
 EN-B contains 6-9% P, 0.5 and 1.0 mil thick  
 EN-C contains 10-12% P, 0.5 and 1.0 mil thick

Examination of the above data clearly shows a corrosion trend between the three electroless nickel (EN) coatings varying in phosphorous content. For both 0.5 mil and 1 mil thickness (identified by subscripts 1,2), coating C with high P exhibited the least corrosion rates and coatings with low phosphorous indicated the highest corrosion rate. This trend was also confirmed by the long-term salt spray test as described later. Electrolytic nickel plated (EL-Ni) coupons did show low corrosion rates but the tarnish of the deposit indicated surface passive films. Pronounced discolorations and rust spots were also observed for EL-Ni in the neutral salt spray study. The electrochemical data sometimes may be misleading, and direct correlations and confirmation should always be sought by a reliable field test simulating the conditions. The low corrosion rates for electroplated samples are possibly due to formation of passivated films on the surfaces of nickel coated SS301 and phosphor bronze.

Figure 1 depicts a comparative behavior of the Tafel plots for electroless nickel coatings with varying phosphorous (P) contents. The open circuit potentials for these coatings varied from  $-0.250$  to  $-0.300$  V . The cathodic arms of these curves seemed to indicate diffusion limited currents which tend to increase with potential changes.

Figure 2 shows the corresponding Potentiodynamic Polarization Plots (PDP) which serve as representative fingerprints of these coatings. A detailed examination of these plots shows the potential ranges where these have the tendency to corrode the most and where these are prone to passivation. In these curves, anodic branches extend over a wide potential range and phenomenon is complex. The primary passivation potentials (EPP) for medium and high P coatings are similar and breakdown potential (Eb) are different and the passive regions are different. The coating with low P exhibits high currents in the active region thus yielding higher corrosion rates. The width of the passive region is useful for characterizing the corrosion trend. The pitting tendency may also be evaluated and will be dealt with under cyclic polarization plots. At extreme anodic potentials beyond 0.5 V vs. open circuit potential (transpassive region), the coatings tend to dissolve anodically and a green colored solution streak appeared to ooze out from the surface of the active working electrode at these potentials. This is due to the dissolution of metallic contents of the coating resulting in the formation of dirty green precipitates<sup>10</sup> in solution with local changing pH<sup>11</sup> to alkaline values (pH= 9-10). The filtered precipitates changed to brown precipitates due to air oxidation. Analysis of the filtered solution and the precipitates by atomic absorption spectroscopy and solids by

SEM–EDAX confirmed the presence of sizeable amounts of Ni, and Fe, and traces of Cr and Cu . The plausible reaction mechanism may be as given below:



The surface examination of these coupons after anodic potentiodynamic polarization curves by SEM indicated dissolution of coating resulting in peels, oxidation of surface and preferential pitting depending on the substrate. Figures 3- 5 depict their secondary electron images of overall surfaces and surface morphology after PDP plots.

### Cyclic Polarization

Figure 7 depicts the cyclic polarization Plot (CPP) of high phosphorous electroless nickel in 5% NaCl. The standard procedure for conducting this test is described in ASTM Standards annual book.<sup>12</sup> The anodic scan shows

some negative hysteresis with a new repassivation potential, ( $E_{rp}$ ) but it appears that the film is transient and unstable showing a double loop cathodic to  $E_{rp}$  with higher corrosion currents. A significant variation (about 500 mvs) between  $E_{pp}$  and  $E_{rp}$  was observed.

The behavior of the same coating (High P-EN) after annealing at 400°C for 72 hours (Figure 8) was different. The reverse anodic scan showed enhanced negative hysteresis but the difference between  $E_{rp}$  and  $E_{pp}$  diminished after heating treatment, yielding lower corrosion currents. It seems that the annealed coating improved in corrosion performance as indicated by the decrease in corrosion currents. The annealing process followed by cooling to ambient temperature brings structural changes by shrinkage, which tends to improve corrosion resistance. The effect was not pronounced if the coating was subjected to 150 °C. It has been mentioned in literature<sup>13</sup> that corrosion resistance was enhanced if heat treatment was done at temperatures > 600°C, which also improved the bonding of coating to steel surfaces. However, one must be cautious about the possibility of micro-cracking during the thermal treatment and shrinkage process.

**Effect of Annealing**

EN plated samples of varying P content were heated at 150°C for a period of 72 hours . No subtle differences in morphology of these coupons and unheated specimens were found by SEM microphotographs. However, some changes were noticed after prolonged heating at 400° C and this effect is discussed under cyclic polarization plots. Since improved corrosion resistance was noticed with deposits containing high phosphorous, all additional work was done only on this coating.

**Effect of Sodium Chloride Concentration**

Table II summarizes the results of varying sodium chloride concentration for high phosphorous- EN coating. All solutions were prepared in de-ionized water and no attempt was made to alter the pH.

**Table II**

Sodium Chloride at Varying Concentrations  
High Phosphorus EN/ SS 301, 0.5 mil

Conc M	$E_{corr}$ , V vs. Ag/AgCl	Corrosion Current, $\mu A$	Corrosion Rate,mpy
0.10	-0.185	0.96	0.41
0.85	-0.224	0.85	0.39
1.00	-0.220	1.01	0.43
2.00	-0.207	0.90	0.38
3.00	-0.239	0.48	0.20
4.00	-0.273	2.03	0.86

The corrosion potential in dilute NaCl shifted to more positive potential which may due to increased solubility of oxygen in dilute electrolyte. The solubility of oxygen decreases with increase in electrolyte concentration. The corrosion potential shifted to more cathodic magnitude at 4M NaCl concentration. With increasing salt concentrations, no major differences in corrosion rates could be detected by Tafel plots.

**Corrosion Studies in Other Electrolytes**

Table III summarizes the corrosion data on High P- EN coatings in diverse electrolytes in order to explore any drastic differences, if any. A few typical plots in the presence of these electrolytes are shown in figures 9-12.

Examination of Table III reveals a few interesting results. In highly oxidizing solutions such as 5% sodium hypochlorite and 1M ammonium persulfate, the corrosion potential,  $E_{corr}$  were shifted to more anodic values. Also, substantial corrosion rates were registered. Metals tend to get oxidized in the presence of hypochlorite and the metal ions thus formed are known to decompose sodium hypochlorite catalytically.<sup>14,15</sup>

Nickel is also attacked by hypochlorite solution producing local pitting. Ammonium persulfate tends to produce sulfuric acid on hydrolysis in aqueous solutions which is corrosive to EN coatings. Neutral salt solutions prove to be less corrosive. Moderate corrosion rates were observed in 1M mineral acids. In presence of reducing hypophosphite medium, the  $E_{corr}$  shifted to more cathodic values and yielded very low corrosion rates. Chlorides and nitrates are soluble, thus they offer little or no film formation protection. Carbonates may form an insoluble corrosion product.

**Table III**

Corrosion of High P Electroless Nickel/SS 301 in Various Electrolytes

Electrolyte	$E_{corr}$ , V vs. Ag/AgCl	Corrosion Current, $\mu$ A.	Corrosion Rate, mpy
1 M Na <sub>2</sub> CO <sub>3</sub>	-0.207	13.6	5.8
5 % NaOCl	0.874	32.5	13.8
1M Na <sub>2</sub> H <sub>2</sub> PO <sub>2</sub>	-0.355	0.1	0.1
1M (NH <sub>4</sub> ) <sub>2</sub> S <sub>2</sub> O <sub>8</sub>	0.351	54.2	23.0
1M NH <sub>4</sub> Cl	-0.172	1.70	0.72
1M Na <sub>2</sub> SO <sub>4</sub>	-0.136	1.8	0.8
1M NaNO <sub>3</sub>	-0.115	2.2	0.9
1M HCl	-0.02	2.7	1.2
1M HNO <sub>3</sub>	0.014	1.9	0.8
1M H <sub>2</sub> SO <sub>4</sub>	0.005	3.7	1.6
1M NaOOCCH <sub>3</sub>	-0.260	1.0	0.4

### Effect of pH

Table IV enlists the corrosion behavior in sodium chloride solutions of varying pH values. At higher pH, the corrosion potential shifted to more cathodic direction and the least corrosion rate was observed. Sodium chloride at very low pH acts as an aggressive corrodant.

**Table IV**

High P- EN Coating in 5% NaCl of Varying pH

pH	$E_{\text{corr}}$ , V vs. Ag/AgCl	$I_{\text{corr}}$ , $\mu\text{A}$	Corr. Rate, mpy
1.5	-0.236	19.9	8.5
6.8	-0.224	0.9	0.4
12.0	-0.429	0.9	0.4

### Galvanic Studies

Nickel plating is more anodic compared to stainless steel and phosphorous bronze substrates. A study of different galvanic couples was initiated in order to understand the role of galvanic corrosion ( Table V).

**Table V**

Couple Vs. SS301	$E_{\text{corr}}$ , V Vs. Ag/AgCl	$I_{\text{corr}}$ , $\mu\text{A}$	Corr. Rate, mpy
EN-Low P	0.104	5.6	2.4
EN-Med P	0.101	7.2	3.2
EN-High P	0.074	2.4	1.1

Changes in P content did not show appreciable differences in electrode potentials. These results are in concurrence with the observations reported by Duncan and Arney .<sup>16</sup>

### B) Salt Spray Studies

Coupons with low, medium and high phosphorous electroless nickel coatings on SS 301 and Phosphor bronze 510 with 0.5 and 1.0 mil coating thicknesses were exposed to neutral salt spray (NSS). Examination of surfaces after 48 hours of exposure indicated no corrosion except light discolorations, and light salt spots. After 500 hours of salt spray exposure, several rust and green spots were observed on the coupons with 0.5 mil thickness of low and medium phosphorous EN. The severity of attack decreased with increasing thickness (1.0 mil ). No distinct difference was found between SS 301 and phosphor bronze substrates. Among the whole group, samples with high phosphorous exhibited the least corrosion except some blotchy discolorations and salt marks. No change in coupon weights was recorded, indicating no attack. These observations are in agreement with the electrochemical data. The corrosion rates observed were the least in coatings containing the highest P

content. The electroplated coupons responded poorly with appearance of numerous rust spots and registered an increase in weight. On some coupons, the coating peeled showing adhesion failure. The electroplated samples showed more porosity by ferroxyl test than the high P- EN samples.

The corrosion resistance of electroless nickel is primarily due to low porosity of the coatings and the inherent tendency of Ni to resist corrosion in many liquids, salts, and atmospheric conditions. Due to the absence of grain boundaries and its amorphous nature in microstructure with high homogeneity, the EN coatings displayed lesser corrosion. These experiments have shown that stainless steel parts resist pitting in the presence of EN coatings in chloride solutions. In order to achieve the desired corrosion resistance, factors such as substrate composition, structure and surface finish played a dominant role. For these SS parts, the original substrate needed electropolishing, deburring in a suitable medium, and alternate cathodic and anodic electrocleaning<sup>17</sup> prior to EN coating. These pretreatments were extremely essential in achieving the desired adhesion, finish, and subsequently qualified a harsh 500 hour salt spray test.

## **Conclusions**

1. Electroless nickel coatings showed a lower porosity compared to electroplated specimens. EN coatings were more uniform with continuous thicknesses compared to equivalent electroplated nickel coatings. This surface property was instrumental in providing better corrosion protection.
2. The integrity, adhesion and corrosion resistance of high phosphorous EN was found to be the highest, and only a few rust spots were observed over the entire surfaces after 500 hours of NSS. On the other hand, the electroplated coupons failed with abundance of rust spots and even peeling of deposits.
3. Electrochemical corrosion rates supported the conclusion that high P deposit was highly corrosion resistant. The data on electroplated samples appeared anomalous due to the presence of passivated films.
4. Heat treatment of samples at 150 °C did not cause any significant change in corrosion resistance whereas changes at 400 °C were noticeable.
5. Galvanic coupling experiments indicated small potential differences which were responsible for small corrosion rates.

## **Acknowledgements**

The author expresses his sincere thanks to Mr. Tom Moyer for providing funding, equipment and

encouragement with his valuable comments for this research and to Mr. Ron Boyer for providing laboratory facilities. Support efforts of the Corporate Product Test Laboratory at Valley Green are also sincerely appreciated.

## **References**

1. Standard Reference Method for Making Potentiostatic and Potentiodynamic Anodic Polarization Measurements, ASTM G5-94, ASTM 100 Barr Harbor Drive, West Conshohocken, PA
2. Standard Practice for Preparing, Cleaning, and Evaluating Corrosion Test Specimens, ASTM G1-90/94.
3. Standard Practice for Operating Salt Spray (Fog) Apparatus, ASTM B117-95.
4. Standard Practice for Laboratory Immersion Corrosion Testing of Metals, ASTM G31-72/1995
5. J. Tafel, Z. Phys. Chem., 50, 641, (1904).
6. M.G. Fontana and N.D. Green, *Corrosion Engineering*, McGraw-Hill and Co., New York, NY, 1967.
7. M.Stern & A. L. Geary, J. Electrochem. Soc. 104, 33-63 (1957).
8. C. Wagner & W. Traud, Zeitschrift fur Electrochemie, ZEELA, 44, 391, (1938).
9. Standard Guide For Conducting and Evaluating Galvanic Corrosion Tests in Electrolytes, ASTM G71-81, 1998.
10. N. Sato, J. Electrochem. Soc., 129, 260 (1982)
11. J.R. Galvane, J. Electrochem Soc., 123, 464, (1976)
12. Standard Test Method for Conducting Cyclic Potentiodynamic Polarization Measurements for Localized Corrosion Susceptibility of Iron-, Nickel-, Cobalt- based Alloys, ASTM Method G 61-86 , 1998.
13. Glenn O . Mallory and Juan B Hajdu, Editors, *Electroless Plating, Fundamentals & Applications*, American Electroplaters & Surface Finishers Society, Orlando, Florida, 1990.
14. K.B. Saubestre and J. Hajdu, Proc. Surface ,66, 192 (1966).
15. A. K. Jing, & N.J. Rao, IPPTA, Vol. 3, No. 7, p. 1, (1991).
16. S. Henrikson, “ Field Tests with metallic materials in Finish, Norwegian and Swedish bleach plants”, 4<sup>th</sup> International Symposium on Corrosion in Pulp and Paper Industry, Stockholm, NACE, p. 128, 1983.
17. R. N. Duncan and T. L. Arney, *Plating and Surface Finishing*, 10, 60, (1989).

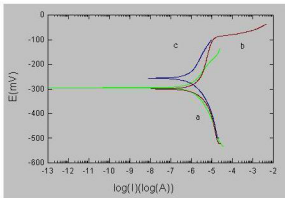


Figure 1 Tafel Plots for Electroless Ni (0.5 mil)/SS 301 in 5% NaCl  
 a - High P      b - Medium P      c - Low P

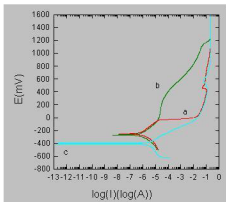
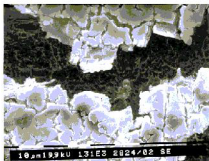
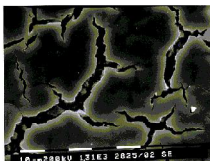


Figure 2 Potentiodynamic Polarization curves of electroless Ni (0.5 mil) /  
 SS 301 in 5% NaCl  
 a - High P      b - Medium P      c - Low P



B



C



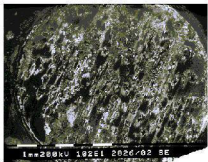
A

Fig 3 Secondary electron images of EN-low P (0.5 ml) / SS 301 after Potentiodynamic Polarization in 5% NaCl

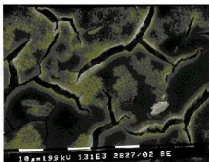
A - Overall Surface

B - Light area

C - Dark area



A

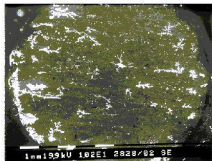


B

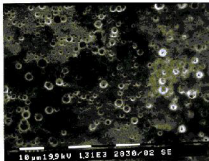
Fig 4 Secondary electron images of EN-medium P (0.5 ml) / SS 301 after Potentiodynamic Polarization in 5% NaCl

A - Overall Surface

B - Typical Surface Morphology



A

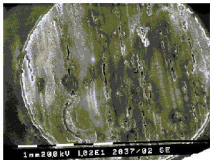


B

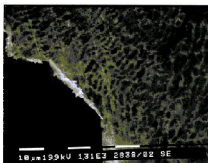
Fig 5 Secondary electron images of EN-high P (0.5 ml) / SS 301 after Potentiodynamic Polarization in 5% NaCl

A - Overall Surface

B - Typical Surface Morphology



A



B

Fig 6 Secondary electron images of electroplated Ni (0.5 ml) / SS 301 after Potentiodynamic Polarization in 5% NaCl

A - Overall Surface

B - Typical Surface Morphology

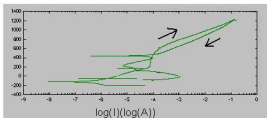


Figure 7 Cyclic Polarization of Electroless Ni High P in 5% Sodium Chloride (0.5 ml) / SS 301 as plated

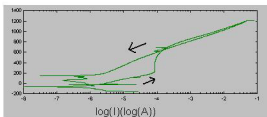


Figure 8 Cyclic Polarization of Electroless Ni High P in 5% Sodium Chloride (0.5 ml) / SS 301 after heating at 400C

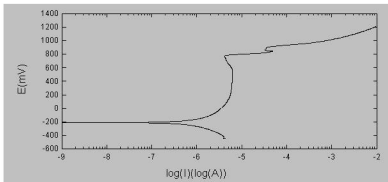


Figure 9 Potentiodynamic Polarization plot of High P-EN in 1 M Sodium Carbonate

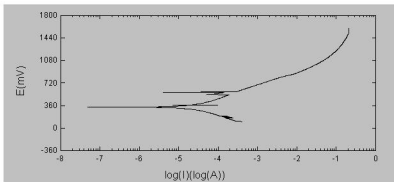


Figure 10 Potentiodynamic Polarization plot of High P-EN in 1 M Ammonium Persulfate

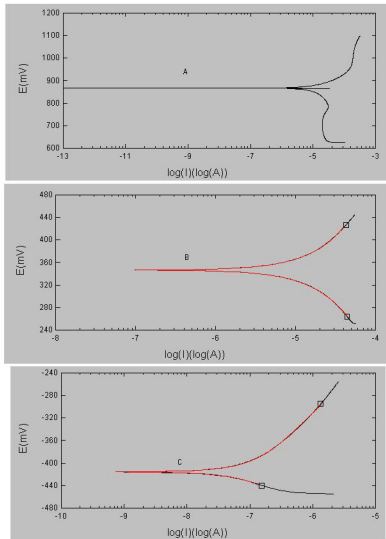


Figure 11 Tafel Plots of High P-EN in (A) 5% Sodium Hypochlorite  
 (B) 1 M Ammonium Persulfate (C) 1 M Sodium Hypophosphite

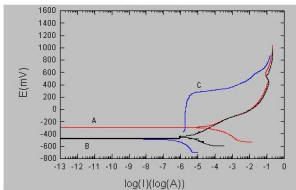


Figure 12 Potentiodynamic Polarization Plots for Med P-EN in 5N NaCl of varying pH (A) 1.5 (B) 6.8 (C) 12.0